Scientific Research Publishing

Open Journal of Earthquake Research, 2025, 14(2), 67-84
https://www.scirp.org/journal/ojer
ISSN Online: 2169-9631
ISSN Print: 2169-9623

Meteorological Anomalies Based on Ground-Based AMeDAS Data for the 1995 Kobe Earthquake: Critical Natural Time Analysis

Masashi Hayakawa[1,2*], Stelios M. Potirakis[3,4,5], Shinji Hirooka[6,7], Yasuhide Hobara[8,9]

[1]UEC Alliance Center, Hayakawa Institute of Seismo Electromagnetics, Co., Ltd. (Hi-SEM), Tokyo, Japan
[2]Advanced Wireless & Communications Research Center, The University of Electro-Communications, Chofu, Japan
[3]Department of Electrical and Electronics Engineering, Ancient Olive Grove Campus, University of West Attica, Athens, Greece
[4]Institute for Astronomy, Astrophysics, Space Applications and Remote Sensing, National Observatory of Athens, Metaxa and Vasileos Pavlou, Athens, Greece
[5]Department of Electrical Engineering, Computer Engineering and Informatics, School of Engineering, Frederick University, Nicosia, Cyprus
[6]HiSR Lab LLC, Tokyo, Japan
[7]Graduate School of Science, Chiba University, Chiba, Japan
[8]Department of Computer and Network Engineering, The University of Electro-Communications, Tokyo, Japan
[9]Center for Space Science and Radio Engineering, The University of Electro-Communications, Tokyo, Japan
Email: *hayakawa@hi-seismo-em.jp, spoti@uniwa.gr, hirooka@hrl.jp, hobara@ee.uec.ac.jp

How to cite this paper: Hayakawa, M., Potirakis, S.M., Hirooka, S. and Hobara, Y. (2025) Meteorological Anomalies Based on Ground-Based AMeDAS Data for the 1995 Kobe Earthquake: Critical Natural Time Analysis. *Open Journal of Earthquake Research*, **14**, 67-84.
https://doi.org/10.4236/ojer.2025.142006

Received: March 17, 2025
Accepted: April 27, 2025
Published: April 30, 2025

Abstract

Two meteorological quantities of *T/Hum* (*T*: temperature and *Hum*: relative humidity) and *ACP* (atmospheric chemical potential) of water molecules based on the "ground-based" AMeDAS (automated meteorological data acquisition system) "open" data of Japan Meteorological Agency have been utilized to explore a possibility of short-term earthquake (EQ) prediction. The target EQ is the famous 1995 Kobe EQ with magnitude of 7.3 on 17 January, 1995. Midnight (LT = 01 h) data of temperature and humidity at a particular station of Kobe, close to the EQ epicenter, have been analyzed, and we have found that there exists only a single and conspicuous peak in both quantities of *T/Hum* and *ACP* on the same day of 10 January, 1995 during the short-term EQ prediction window of one month before and two weeks after an EQ. Fortunately, during this short-term EQ prediction period, the geomagnetic and solar activity was extremely quiet, and so we think that the anomaly on this particular day, just one week before the EQ, is very likely to be a precursor

to the EQ. Then, in order to find any definite causality relationship of this meteorological anomaly to the EQ, we have performed the critical analysis for the same datasets. We have applied the natural time (NT) analysis method to the daily-valued quantities of *ACP* and detrended *T/Hum*, and the NT analysis results revealed criticality in both quantities ~3 weeks before the 1995 Kobe EQ. This implies that the meteorological anomalies as a proxy of the exhalation of radon and charged aerosols from the lithosphere into the atmosphere are at the critical stage ~3 weeks before the EQ and so an anomaly in two meteorological quantities appeared one week before the EQ as a definite precursor to the EQ as suggested by this criticality.

Keywords

Earthquake (EQ) Precursors, AMeDAS Data, Meteorological Parameters, Temperature/Humidity, ACP (Atmospheric Chemical Potential), Statistical Analysis, Critical Analysis, Natural Time (NT) Analysis

1. Introduction

Even though predicting an impending earthquake (EQ) with lead time of about a week or so is highly desired by the general public in order to save human lives and economical losses, this short-term EQ prediction is still a challenging subject left in the field of geophysics. The current topic of the field of seismo-electromagnetics (or short-term EQ prediction), is the elucidation of lithosphere-atmosphere-ionosphere coupling (LAIC), because the ionosphere is found to be very sensitive to pre-EQ lithospheric activity due to the strong coupling among the three regions from the lithosphere to atmosphere and ionosphere (e.g., [1]-[5]). The bottom part of the LAIC is the lithosphere and Earth's surface, and so the information in these bottom regions plays an essential role in these LAIC studies.

Earth's surface monitoring (or remote sensing) from satellites has been extensively performed in order to find any significant precursors to EQs since the pioneering papers by [6]-[9], especially Tronin *et al.* (2002) [9] have found significant temperature increases in and around the relevant fault regions of EQs. Then, many papers have been published so far, to study different physical parameters, including meteorological parameters (temperature, humidity etc.), OLR (outgoing longwave radiation), SLHF (surface latent heat flux) etc. [10]-[26]. Of course, we understand that the main stream of seismo-electromagnetics is the elucidation of the LAIC process, so the information of Earth's surface or near-Earth information is of essential significance as the bottom region of LAIC, because the driving agent of this LAIC is highly likely to lie within the lithosphere [27]-[40].

Those satellite observations in many previous papers [27]-[40] are all based on "open" data from different satellite sources, but the present paper proposes the use of ground-based "open" data with higher temporal and spatial resolution than the satellite remote sensing observations. The data used in this paper are available

from AMeDAS (automated meteorological data acquisition system) of Japan Meteorological Agency (JMA). In our companion paper [41], we have proposed the two physical quantities of T/Hum (T: temperature and Hum: relative humidity) and ACP (atmospheric chemical potential) of water molecules as a short-term EQ predictor. We have analyzed those quantities for the first time for the famous 1995 Kobe EQ (M = 7.3), in order to examine whether these two physical quantities themselves are a powerful tool as a possible candidate of short-term EQ prediction or not, in addition to LAIC studies, and succeeded in identifying a clear anomaly in both quantities, just one week before the EQ. Because we have found a significant precursory anomaly for this particular EQ, we will here perform the criticality analysis as the next step. An important direction in the field of possible seismic precursors is the application of critical analysis to various quantities possibly involved in LAIC. Such studies have revealed that different layers of LAIC reach a critical state before a strong EQ. Specifically, the criticality analysis method called "natural time" (NT) analysis has successfully been applied to VLF subionospheric propagation data, ULF magnetic field data, global navigation satellite system deformation (GNSS) data, surface latent heat flux (SLHF) data and very recently in stratospheric potential energy (E_p), as well to other EQ-related observables such as pre-EQ seismic electric signals (SES), foreshock seismicity, MHz fracture-induced electromagnetic emissions (FEME) recording (e.g., [42]-[50]).

The rest of this paper is organized as follows. Section 2 presents the target EQ, AMeDAS data, and solar-geomagnetic conditions. In Section 3, we review our meteorological quantities, whereas Section 4 presents the conventional statistical analysis using the confidence bounds and its results. Section 5 presents the most important part of this paper on the NT analysis and its results. Sections 6 and 7 are the discussion and conclusion, respectively.

2. EQ Studied in This Paper, and Solar, Geomagnetic Activity

2.1. Target EQ and AMeDAS Stations

The target EQ of this paper is the famous 1995 Kobe EQ that happened at 5 h 46 m (JST, local time (LT)) on January 17, 1995, having its epicenter at the geographical coordinates (34˚35.9'N, 135˚02.1'E), as shown in **Figure 1**, with a magnitude $M = 7.3$, and with a depth of 16 km. We have plotted a few AMeDAS meteorological stations (black boxes) close to the EQ epicenter together with the fault regions (Rokko/Awaji island faults) possibly related with this EQ.

2.2. Solar-Geomagnetic Environment

Figure 2 illustrates the temporal evolutions of the geomagnetic activity (Dst and Kp indices) and the solar radiation flux at the wavelength of 10.7 cm (f10.7) during the period of 1 May, 1994 through 31 May, 1995 (over one year) including the day of the EQ. We think that unlike the ionosphere, the meteorological parameters studied in this paper are likely to be much less influenced by solar-geomagnetic conditions and perturbations. As seen from the plot of Dst (**Figure 2**)

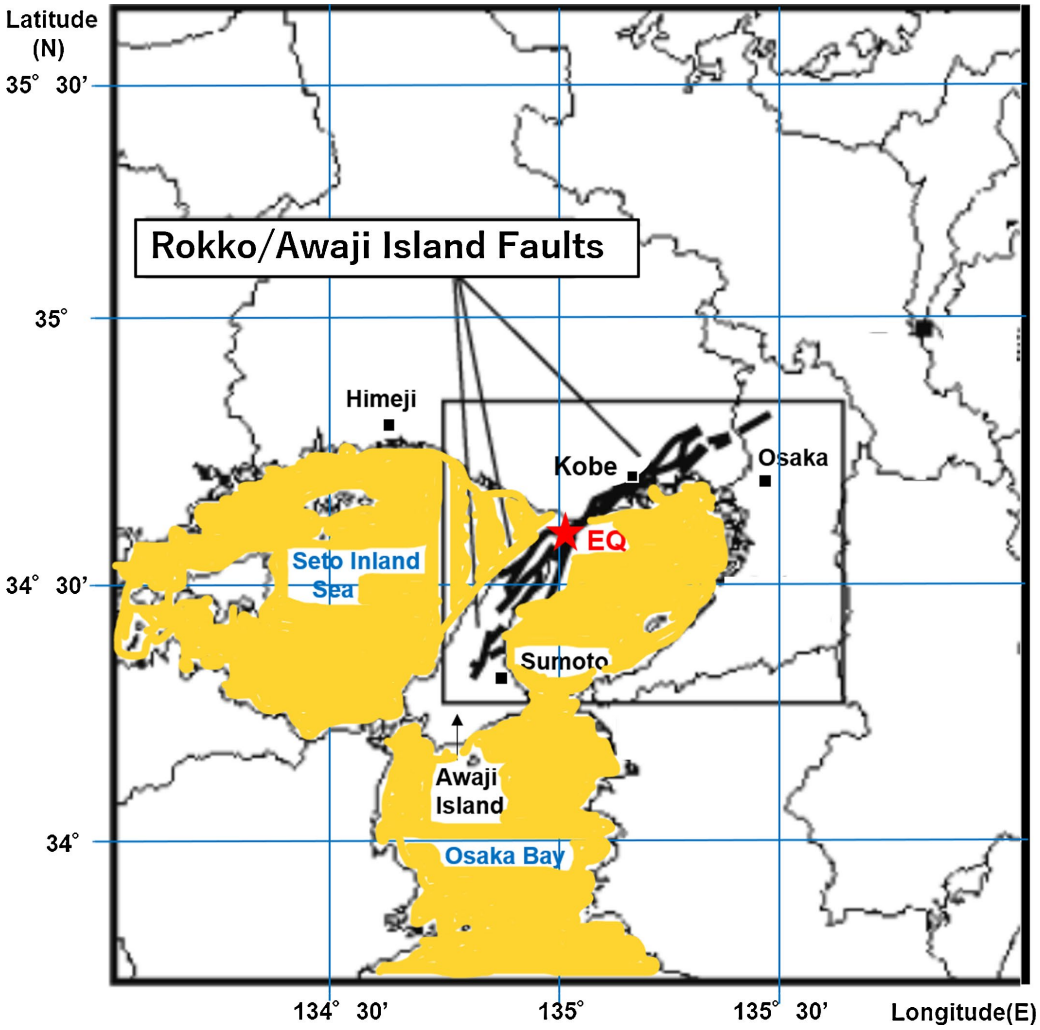

Figure 1. Location of the epicenter of the 1995 Kobe EQ (indicated by a red star) and some AMeDAS stations (shown as black boxes) including Kobe. Also, the possible fault regions are plotted by bold lines, and sea parts are given in brown.

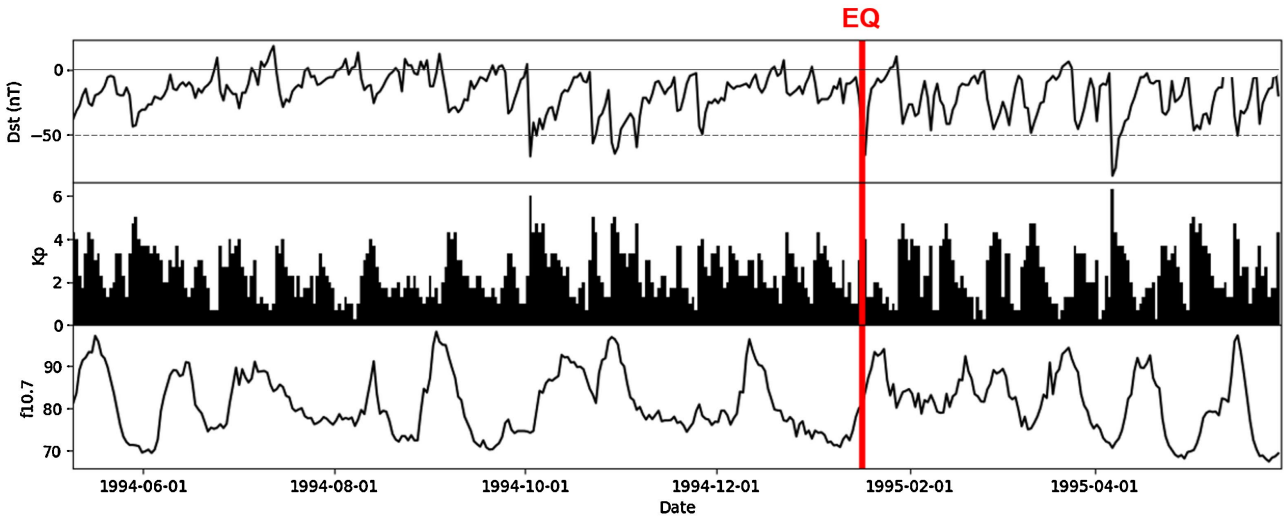

Figure 2. Temporal evolutions of geomagnetic activity (Dst and Kp indices) and solar radiation flux (f10.7) during the period of 1 May 1994 to 31 May 1995. The time of the 1995 Kobe EQ is indicated by the vertical red line.

some geomagnetic disturbances with Dst below –50 nT are only noticed in October and November, 1994, but the geomagnetic activity after the beginning of December, 1994 till the day of the EQ, which is very important for the short-term EQ prediction, was extremely quiet, because Dst is less than –20 nT. Further, the solar radiation flux (F10.7) as an indicator of overall solar activity levels was also found to be less than 100. Taking into account the quiet solar-terrestrial conditions just before the EQ, we are ready to investigate short-term EQ precursors within the short-term EQ prediction span of one month before and two weeks after the EQ.

3. Meteorological Parameters from the Japanese AMeDAS Data

When thinking of a possible short-term EQ predictor, we try to use the openly available data from ground-based observations of meteorological parameters. Even though there have recently been published many papers on the study of these meteorological parameters such as temperature, humidity, etc. from the "open" data of satellite remote sensing observations [6]-[40]. So, our companion paper [41] is the first attempt to use the ground-based open data. Before going to the critical analysis, we are obliged to describe the data and analysis results [41] briefly again in this paper, for completeness reasons.

3.1. AMeDAS Data

JMA has established an AMeDAS since 1975, and it has been in operation very regularly. Four meteorological parameters are being measured at each station: 1) precipitation (or rainfall) (in units of 0.5 mm), 2) air temperature (in units of 0.1˚C) and air relative humidity (in %), 3) sunshine duration, and 4) wind direction/speed, and this AMeDAS network includes as many as 1300 stations all over Japan, so the stations are located, on average, with an interval of 17 km.

3.2. Meteorological Parameters Used in This Paper

We have studied the following two meteorological quantities proposed in Hayakawa *et al.* (2022) [34] and Schekotov *et al.* (2023) [51]. The fundamental idea may be that radon (Rn) rises to the Earth's surface more intensely along seismic faults or volcanic fumaroles during the EQ preparation phase, and the subsequent air ionization leads to a decrease in the air humidity and an increase in its temperature [51]. So, the first quantity of our interest is the simple ratio of temperature, T (in ˚C) to humidity (relative humidity), Hum (in %), *i.e.*, T/Hum, because of our expectation of an enhanced seismogenic effect of increasing T and decreasing Hum. The second quantity is ACP (atmospheric chemical potential) which is given by the following equation [2]:

$$ACP(\text{in eV}) = 5.8\times10^{-10}\left(20T+5463\right)^2 \ln\left(100/Hum\right) \quad (1)$$

Here we indicate the reason why we call this the chemical potential. Because at

the moment of water molecule condensation/evaporation or attachment/detachment to the ions, the latent heat release/absorption is equal to the chemical potential [5]. This ACP value is supposed to yield an increase during the process of air ionization by any agents including galactic cosmic rays etc., one of them being by the exhalation of radon (Rn) and charged aerosols which is known to be released during the pre-EQ enhancement as reported by several workers (e.g., [52]-[56]).

We have analyzed the data from some other AMeDAS of stations near the EQ epicenter in the western part of Japan: Kobe (34˚41'N, 135˚12'E), Osaka (34˚41'N, 135˚31'E), Sumoto (34˚19'N, 134˚51'E), and Himeji (34˚54'N, 134˚40'E) as indicated by black boxes in **Figure 1** and we have confirmed the presence of the same anomalous day at all of these stations. So, in the following, we will present again the results only for one particular station of Kobe from [41] as a representative example.

4. Statistical Analysis Based on the Mean and Standard Deviation

4.1. Midnight Data

The basic quantities of T and Hum only around midnight are used, and we choose LT = 01 h because daytime is strongly influenced by strong solar radiation and we think that the time period around midnight is considered to be most suitable for our analysis by excluding this solar effect.

4.2. Conventional Statistical Results

We will first repeat the statistical results from [41]. **Figure 3(a)** is the temporal evolution of the detrended daily value of T/Hum (*i.e.*, $\delta(T/Hum)=(T/Hum)-m$ (where m is the running mean during the previous 30 days), and the standard deviation of σ is also estimated during the previous 30 days, as followed by Hayakawa *et al.* (2022) [34]. Each vertical black bar indicates the current value for each day and the abscissa indicates the date. The day of EQ (17 January, 1995) is indicated by a vertical red line. When there is no vertical bar on a particular day, it means that the current value is below the means value of m. There are plotted three curves in the figure; the bottom green curve refers to $m+\sigma$, the orange curve to $m+2\sigma$, and the red curve to $m+3\sigma$. The period of presentation in **Figure 3** is a time window of about one month before and a few weeks after an EQ as short-time EQ prediction window. Now we will try to identify any anomalous variations by using the confidence bounds with m and σ. In our previous works it has been taken a criterion of $m+2\sigma$, as it is usually done when dealing with different physical parameters (e.g., [3]), but in this paper we adopt a much more severe criterion of $m+3\sigma$ as used conventionally in the field of astrophysics. **Figure 3(a)** indicates that we can notice a single and a very remarkable peak exceeding $m+3\sigma$ only on 10 January, 1995, just one week before the EQ. Other weather effects (such as storm, fog, etc) could not influence this anomaly.

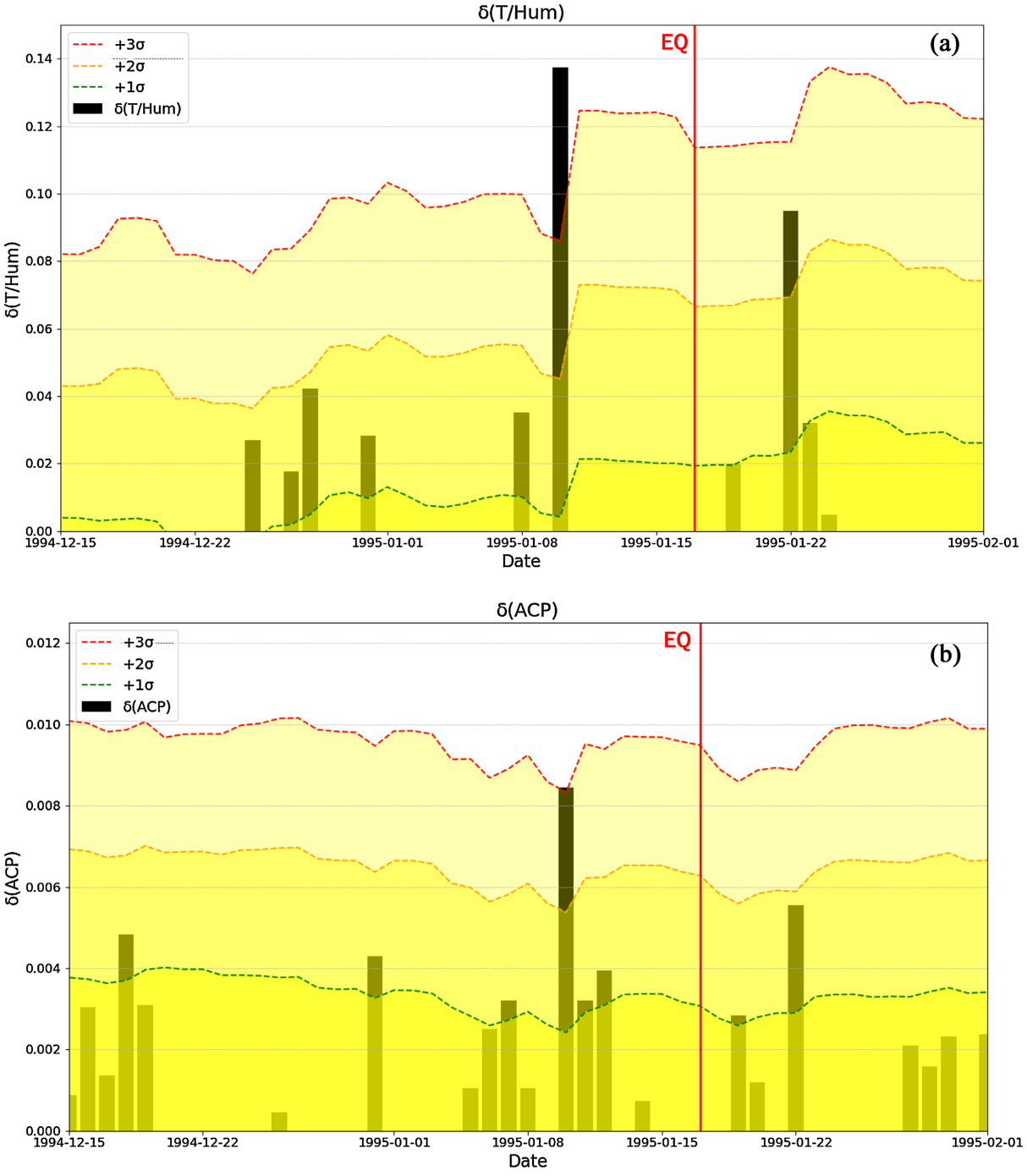

Figure 3. Temporal evolutions of daily values (vertical black bars) of (a) detrended T/Hum, $\delta(T/Hum)$, and (b) detrended $ACP, \delta(ACP)$, during a short-term EQ window of about one month before and a few weeks after the EQ. A vertical red line indicates the day of the EQ. Three colored curves: bottom green curve refers to $m+\sigma$, orange to $m+2\sigma$, and red to $m+3\sigma$. An anomalous day is clearly noticed on 10 January, 1995.

Now we move on to **Figure 3(b)** for the plot of detrended ACP, *i.e.* $\delta(ACP)$. Quite similarly as in **Figure 3(a)**, we can identify the same anomaly on the same day in **Figure 3(b)**. Its anomalous value is not exceeding this criterion of $m+3\sigma$, but stands out well above $m+2\sigma$. This peak is again the only one within the

short-term EQ prediction window.

Finally, we can conclude that the significant peaks in the two parameters, as seen in **Figure 3(a)** and **Figure 3(b)**, both appear on 10 January, 1995, just one week before the EQ. Hence, it is highly likely that an anomaly on 10 January, 1995 is a possible precursor to the EQ. Further, we will apply a critical analysis to the same meteorological quantities, T/Hum and ACP, in order to identify whether the above presented peaks are due to the criticality or the causality relationship with this EQ.

5. Natural Time (NT) Analysis

5.1. NT Analysis Method

The NT time series analysis method has initially been applied to the ultra-low frequency (≤1 Hz) seismic electric signals (SES) [57]-[59], and has been shown to be optimal for enhancing the signals in the time-frequency space [60]. The full theoretical details of this method can be found in the monograph by Varotsos *et al.* [42] (and references therein), while the application of NT analysis to various seismo-EM signals has been presented in detail in [46]. Also, recent studies using the NT time series method to other observable quantities of LAIC have shown the existence of critical dynamics before EQs [46]-[48]. In what follows, we will briefly present the key notions of this method and the process of applying it to our meteorological data.

Initially, for a number of N events, we determine the NT of the k-th (in order of occurrence) event as $\chi_k = k/N$, which is actually the order of occurrence normalized in the interval (0, 1]. Next, we determine the "energy" of each event in NT, which is symbolized as Q_k for the k-th event. At this point we have to mention that Q_k corresponds to different kinds of quantities, depending on the time series under analysis. For example, in the case of seismic events Q_k is the seismic energy released (seismic moment), while for the dichotomous SES signals Q_k corresponds to the SES pulse duration [59]. On the other hand, in the case of the fracto-electromagnetic emission signals in the MHz band, which are non-dichotomous signals, Q_k denotes the energy of each event by using consecutive amplitude values above a noise threshold as described in [44].

Then, we study the resulting time series (χ_k, Q_k). The approach of a dynamical system to criticality is identified by means of the variance $\kappa_1 = \langle \chi^2 \rangle - \langle \chi \rangle^2$ of NT, where $\langle f(\chi) \rangle = \sum_{k=1}^{N} p_k f(\chi_k)$, where $p_k = Q_k / \sum_{n=1}^{N} Q_n$ is the normalized energy released during the k-th event. Hence, the quantity κ_1 can be written as $\kappa_1 = \sum_{k=1}^{N} p_k \chi_k^2 - \left(\sum_{k=1}^{N} p_k \chi_k \right)^2$. Moreover, the entropy in NT is defined as $S_{nt} = \sum_{k=1}^{N} p_k \chi_k \ln \chi_k - \left(\sum_{k=1}^{N} p_k \chi_k \right) \ln \left(\sum_{k=1}^{N} p_k \chi_k \right)$ [61]. The entropy in NT is a dynamic entropy, depending on the order of the events [60]. Also, S_{nt-}, the entropy under time reversal, *i.e.*, by reversing the order of the considered events (which of course changes the natural time used for the calculations), is also stud-

ied [61].

In many dynamical systems studied by the NT analysis method, it has been found that the value of κ_1 is a measure to quantify the extent of the organization of the system at the onset of the critical stage [41]. The criticality is reached when (a) κ_1 takes the value $\kappa_1 = 0.07$, and (b) at the same time both the entropy in NT and the entropy under time reversal satisfy the following condition $S_{nt}, S_{nt-} < S_u = (\ln 2/2) - 1/4$ [42] [62], where S_u is the entropy of the uniform distribution in NT [41] [62].

In the special case of NT analysis of foreshock seismicity [57] [59] [61] [63], we study the evolution of the quantities $\kappa_1, S_{nt}, S_{nt-}$, and $\langle D \rangle$ over time, where $\langle D \rangle$ is the "average" distance between the normalized power spectra $\Pi(\tilde{\omega}) = \left| \sum_{k=1}^{N} p_k \exp(j\tilde{\omega}\chi_k) \right|^2$ ($\tilde{\omega}$ stands for the angular frequency in NT) of the evolving seismicity and the theoretical estimation of $\Pi(\tilde{\omega})$ for $\kappa_1 = 0.07$, $\Pi_{critical}(\tilde{\omega}) \approx 1 - \kappa_1 \tilde{\omega}^2$. Moreover, an "event" for the NT analysis of seismicity is considered to be any data point of the original seismicity time series (time series of magnitudes of EQs) that surpasses a magnitude threshold, M_{Thres}.

The analysis starts with an appropriate low threshold and taking into account only an adequate number of, first in the order of occurrence, events. Next, the subsequent events, in their original order, are one-by-one taken into account. For each additional event that is taken into account, the quantity χ_k is rescaled within the interval (0, 1] and all $\kappa_1, S_{nt}, S_{nt-}$, and $\langle D \rangle$ are re-calculated. This way, a temporal evolution of these quantities is obtained. The described procedure is repeated for several, increasing, values of M_{Thres} for each studied geographic area, and everything is repeated for different overlapping areas.

The seismicity is considered to be in a true critical state, a "true coincidence" is achieved, as soon as (a) κ_1 takes the value $\kappa_1 = 0.07$, (b) at the same time for both the entropy in NT and the entropy under time reversal satisfy the condition $S_{nt}, S_{nt-} < S_u$, and three additional conditions are satisfied: (c) The "average" distance $\langle D \rangle$ should be smaller than 10^{-2}, *i.e.*, $\langle D \rangle = \left| \Pi(\tilde{\omega}) - \Pi_{critical}(\tilde{\omega}) \right| < 10^{-2}$ (this is a practical criterion for signaling the achievement of spectral coincidence) [42]; (d) the parameter κ_1 should approach the value $\kappa_1 = 0.070$ "by descending from above", *i.e.*, before the main event the parameter κ_1 should gradually decrease until it reaches the critical value 0.070 (this rule was found empirically) [42] [57]; (e) the above-mentioned conditions (a)-(d) should continue to be satisfied even if the considered M_{Thres} or the area within which the seismicity is studied are changed (within reasonable limits).

The use of the magnitude threshold excepts some of the weaker EQ events (those events that their magnitude is $< M_{Thres}$) from the NT analysis. However, the usage of the magnitude threshold is valid for the reason that some recorded magnitudes are not considered reliable due to the seismographic network. On the other hand, the application of various M_{Thres} values are useful in determining the time range within which criticality is reached. This is because, in some cases, it is found that more than one time-points may satisfy the rest of the NT critical

state conditions (a)-(d), and criterion (e) is the one that finally reveals the true time of criticality.

For the application of NT analysis to the meteorological quantities analyzed in this study, we follow the paradigm of the NT analysis of seismicity. Specifically, in the case of the atmospheric chemical potential (*ACP*) the necessary threshold values are defined in terms of *ACP* values and the "energy" Q_k values are daily *ACP* values exceeding the considered threshold. Similarly, in the case of the temperature over humidity (T/Hum), the positive detrended daily values $\delta(T/Hum)$ are used to define the necessary threshold values and the "energy" Q_k. The detrended daily values are calculated by subtracting the running mean of T/Hum (see Section 4.2 and **Figure 3(a)**) from the T/Hum daily values, in order to remove T/Hum seasonal variation.

5.2. NT Analysis Results

In this section we present the results obtained by the application of the NT analysis method to the daily-valued time series of *ACP* (**Figure 4**) and $\delta(T/Hum)$ (**Figure 5**). We have applied the NT method to the above-mentioned meteorological quantities as explained in Section 5.1. Specifically, for each one of the aforementioned meteorological quantities, we consider as an event any daily value of the meteorological quantity under analysis, that is higher than a certain threshold; that is, we exclude values which are weaker than the specific threshold. Then, the "energy" Q_k of the *k*-th revealed event is considered to be equal to the corresponding daily value of the analyzed meteorological quantity. Finally, the NT analysis is applied to the time series of the revealed events of each meteorological quantity, as in the case of the pre-EQ seismic activity (see [45] [46]).

Figure 4 presents the NT analysis results for the *ACP* time series over a time period of three months from 17 November 1994 to 17 February 1995 (two months before and one month after the occurrence of the 1995 Kobe EQ). As can be seen from **Figure 4**, the NT criticality criteria were satisfied during the time period 23-30 December 1994, since during that time interval, simultaneously, κ_1 approaches the value $\kappa_1 = 0.070$ " by descending from above", $S_{nt}, S_{nt-} < S_u$ and $\langle D \rangle < 10^{-2}$ for all four presented ACP_{Th} threshold values (see also Subsection 5.1). The magenta patches in **Figure 4** show the time intervals during which the approach to criticality was found for each ACP_{Th}, while their intersection reveals that "true coincidence", *i.e.*, true critical state (see Subsection 5.1), was achieved during the time period 23-30 December 1994. This means that critical dynamics are embedded in the *ACP* time series for a time period of 7 days, ~3 weeks before the 1995 Kobe EQ (from 25 days up to 18 days before the EQ occurrence on17 January 1995).

For the $\delta(T/Hum)$ quantity, the NT analysis results are portrayed in **Figure 5**. Similarly, for this meteorological quantity, the NT criticality criteria were satisfied on 27 December 1994, also ~ 3 weeks before the 1995 Kobe EQ. As already mentioned in Subsection 5.1, for the NT analysis of $\delta(T/Hum)$ only the positive values of the $\delta(T/Hum)$ time series were considered as events. Due to

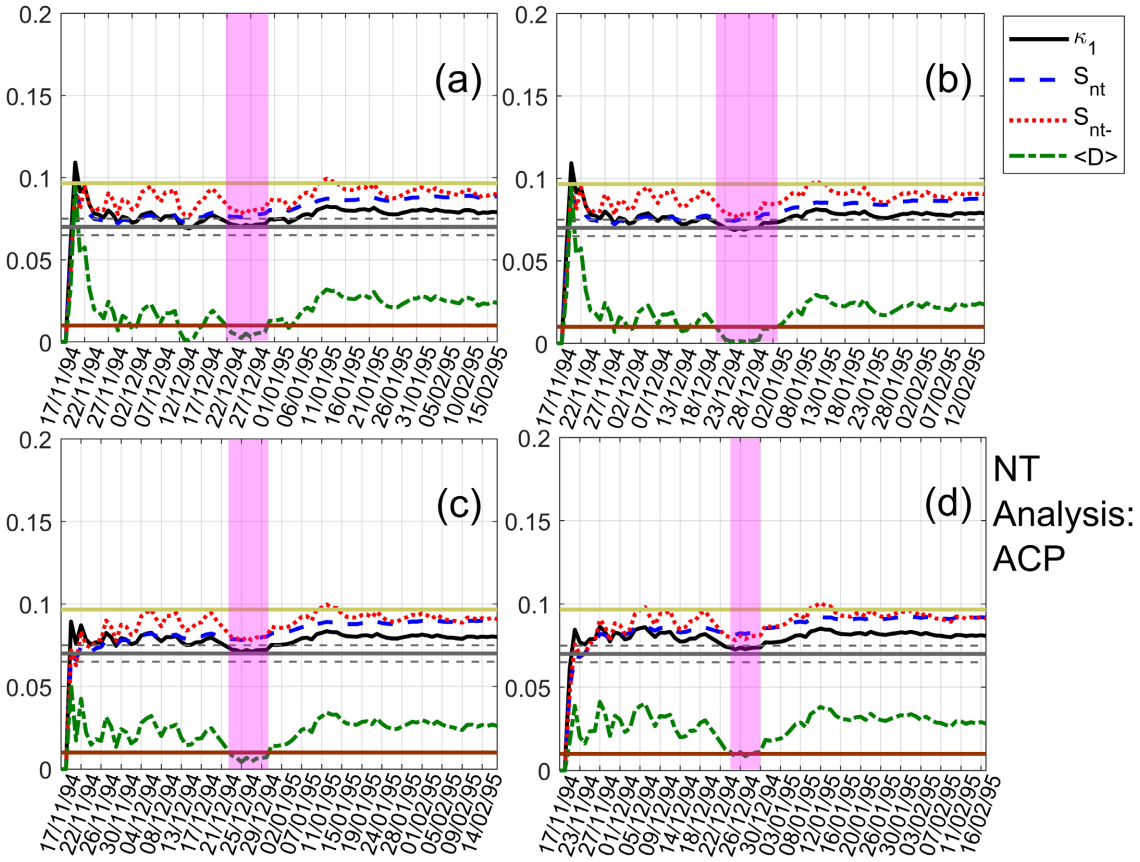

Figure 4. NT analysis of the ACP meteorological quantity time series for the time period from 17 November 1994 to 17 February 1995. The presented temporal variations of the NT parameters correspond to the different thresholds of ACP_{Th} : (a) 0, (b) 0.0014, (c) 0.0021, (d) 0.0035, respectively. The limit value of the entropy $S_u(\approx 0.0966)$ appears as a horizontal solid light green line, while the κ_1 value 0.07 along with a region of ±0.05 around it, are denoted by a horizontal solid grey and two horizontal dashed grey lines, respectively. The 10^{-2} $\langle D \rangle$ threshold is shown as a horizontal brown line. The events presented in each panel depend on the corresponding ACP_{Th} . Moreover, although the conventional time (date) of the occurrence of each corresponding event is noted in the x-axis tick values, the x-axis scale actually follows the NT representation; for this reason, the x-axis is not linear in conventional time.

that, the number of $\delta(T/Hum)$ events during the time period used for the ACP case was quite low for NT analysis. Consequently, in order to increase the number of $\delta(T/Hum)$ events taken into account, the NT analysis of $\delta(T/Hum)$ has been performed for a longer time period than in the ACP case, namely from 17 October 1994 to 17 February 1995 (three months before and one month after the occurrence of the 1995 Kobe EQ).

6. Discussion

In our companion paper [41], we have proposed two meteorological quantities of T/Hum and ACP as a possible candidate of short-term EQ prediction, and we have examined those values especially at midnight that are free from strong solar radiation, for a particular famous 1995 Kobe EQ ($M = 7.3$) on 17 January, 1995. Based on the data during over one year data around the day of EQ, we have found

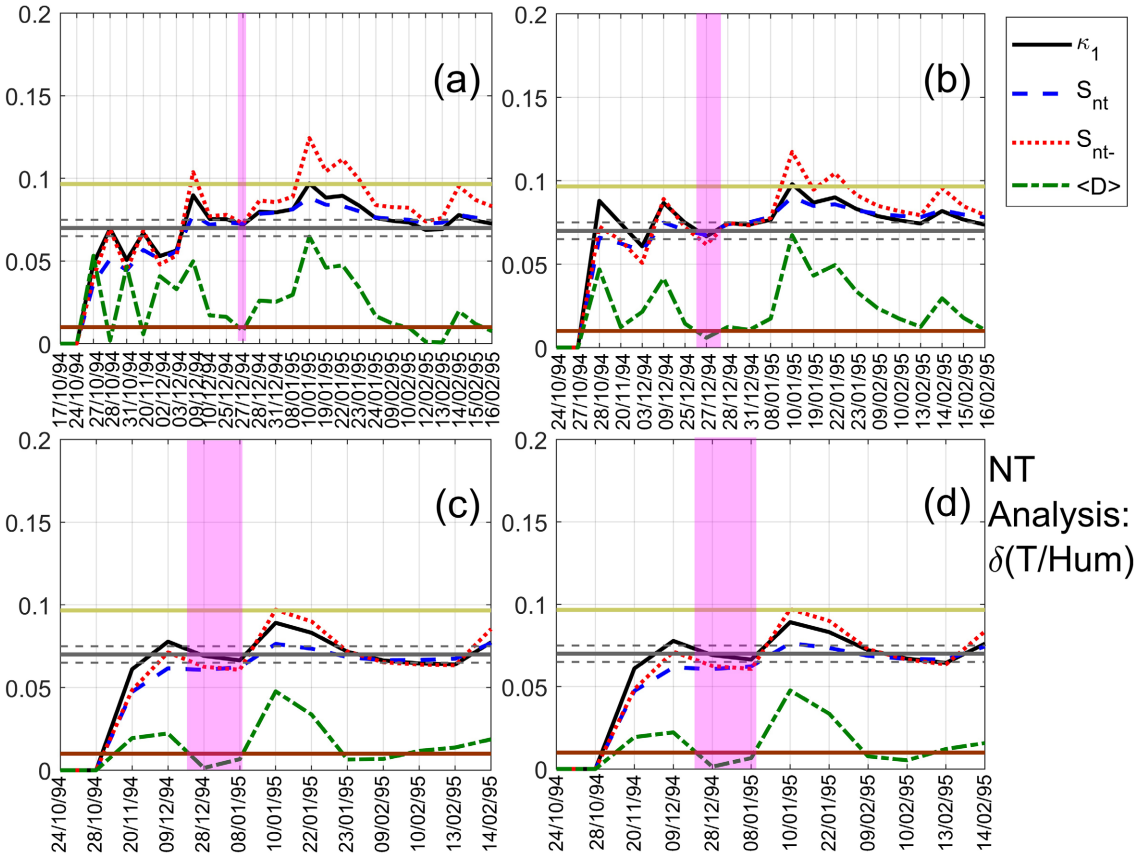

Figure 5. NT analysis of the $\delta(T/Hum)$ meteorological quantity time series for the time period from 17 October 1994 to 17 February 1995. The presented temporal variations of the NT parameters correspond to the different thresholds of $\delta(T/Hum)_{Th}$: (a) 0, (b) 0.015, (c) 0.03, (d) 0.035, respectively. Figure format follows the format of **Figure 4**.

a very conspicuous anomaly on 10 January, 1995, just one week before the EQ in both quantities within the short-term EQ prediction window of one month before and two weeks after an EQ. Specifically, T/Hum exhibited an anomaly exceeding $m+3\sigma$, whereas the corresponding ACP anomaly exceeded $m+2\sigma$. If a meteorological process is ending up to an observed non-seismogenic statistical anomaly, e.g., due to rainfall, this anomaly is not related to a phase transition or a course to an extreme event (in the sense of complex system theory), therefore criticality is not expected to precede. So, we have applied the NT critical analysis to the same two meteorological quantities, and we have found that criticality signatures were clearly identified in both the ACP and the detrended T/Hum ~ 3 weeks before the EQ. So, we can conclude that the observed conspicuous anomaly on 10 January, 1995, just one week before the EQ, is considered to be the consequence of this preceding critical signature observed three weeks before the EQ, and so that this anomaly is highly likely to be a possible precursor to the Kobe EQ. The presence of this critical signature may indicate that these meteorological anomalies can be the possible candidate of seismogenic effects in the lithosphere probably as a proxy to the emanation of radon and charged aerosols during the EQ preparation phase

(*i.e.*, [64]).

7. Conclusions

We will summarize the important results emerged from this work.

1) Based on the data over one year around the 1995 Kobe EQ happened on 17 January, 1995, the statistical analysis using the confidence bounds has found a remarkable anomaly on 10 January, 1995, just one week before the Kobe EQ (within the short-term EQ prediction window) both for the two quantities of T/Hum and ACP. The peak on this particular day exceeded $m+3\sigma$ for T/Hum, and well above $m+2\sigma$ for ACP [41]. This peak on 10 January, 1995 has been confirmed at other stations, providing further confidence on this presence.

2) By applying the critical NT analysis to the same data, we have found critical signatures about 3 weeks before the EQ in both quantities, preceding the above anomaly on 10 January, 1995. So, we can conclude that the statistical anomaly on 10 January, 1995 and the corresponding criticality of 25/12/1994 (ACP) and 23/12/1994 (T/Hum) are highly likely to be due to the EQ preparation. This may suggest that our meteorological quantities reflect the critical state associated with these quantities, probably as the consequence of emanation of radon and charged aerosols during EQ preparation phase, resulting in the notable changes in T and Hum.

3) A combinational use of two quantities of T/Hum and ACP is recommended for the study of short-term EQ prediction, because of taking into account the advantage of each quantity. Unfortunately, the quantity of T/Hum shows a strong seasonal variation, and so it is useful especially during winter-time like the Kobe EQ [41]. On the other hand, the other quantity ACP is found to be a stable EQ predictor and can be utilized during the whole year. This paper has provided quantitative evidence on the usefulness of ACP, which has been recently extensively studied (but unfortunately only qualitatively) [65]-[68].

Acknowledgements

The authors are grateful to the staffs of Hi-SEM and UEC for their extensive support. The AMeDAS data are available from the site of https://www.data.jma.go.jp/risk/obsdl/index.php (accessed on 1 April, 2023), and the data of geomagnetic and solar activities can be downloaded from the OMNIWEB (https://omniweb.gsfc.nasa.gov/form/dx1.html, accessed on 1 January, 2024).

Conflicts of Interest

The authors declare no conflicts of interest regarding the publication of this paper.

References

[1] Hayakawa, M. and Molchanov, O.A., Eds. (2002) Seismo Electromagnetics: Litho-Sphere-Atmosphere-Ionosphere Coupling. Terrapub, 477 p.

[2] Pulinets, S.A. and Boyarchuk, K. (2004) Ionospheric Precursors of Earthquakes.

Springer, 315 p.

[3] Hayakawa, M. (2015) Earthquake Prediction with Radio Techniques. Wiley, 294 p. https://doi.org/10.1002/9781118770368

[4] Ouzounov, D., Pulinets, S., Hattori, K. and Taylor, P. (2018) Pre-Earthquake Processes: A Multidisciplinary Approach to Earthquake Prediction Studies. AGU Geophysical Monograph 234, Wiley, 365 p.

[5] Pulinets, S., Ouzounov, D., Karelin, A. and Boyarchuk, K. (2022) Earthquake Precursors in the Atmosphere and Ionosphere: New Concepts. Springer, 294 p.

[6] Gorny, V.I., Salman, A.G., Troni, A.A. and Shilin, B.B. (1988) The Earth's Outgoing IR Radiation as an Indicator of Seismic Activity. *Proceedings of the USSR Academy of Sciences*, **30**, 67-69.

[7] Qiang, Z.J., Xu, X.D. and Dian, C.G. (1991) Thermal Infrared Anomaly Precursor of Impending Earthquakes. *Chinese Science Bulletin*, **36**, 319-323.

[8] Tronin, A.A. (1996) Satellite Thermal Survey—A New Tool for the Study of Seismoactive Regions. *International Journal of Remote Sensing*, **17**, 1439-1455. https://doi.org/10.1080/01431169608948716

[9] Tronin, A.A., Hayakawa, M. and Molchanov, O.A. (2002) Thermal IR Satellite Data Application for Earthquake Research in Japan and China. *Journal of Geodynamics*, **33**, 519-534. https://doi.org/10.1016/s0264-3707(02)00013-3

[10] Dey, S. and Singh, R.P. (2003) Surface Latent Heat Flux as an Earthquake Precursor. *Natural Hazards and Earth System Sciences*, **3**, 749-755. https://doi.org/10.5194/nhess-3-749-2003

[11] Ouzounov, D. and Freund, F. (2004) Mid-Infrared Emission Prior to Strong Earthquakes Analyzed by Remote Sensing Data. *Advances in Space Research*, **33**, 268-273. https://doi.org/10.1016/s0273-1177(03)00486-1

[12] Surkov, V.V., Pokhotelov, O.A., Parrot, M. and Hayakawa, M. (2006) On the Origin of Stable IR Anomalies Detected by Satellites above Seismo-Active Regions. *Physics and Chemistry of the Earth, Parts A/B/C*, **31**, 164-171. https://doi.org/10.1016/j.pce.2006.02.020

[13] Tramutoli, V., Cuomo, V., Filizzola, C., Pergola, N. and Pietrapertosa, C. (2005) Assessing the Potential of Thermal Infrared Satellite Surveys for Monitoring Seismically Active Areas: The Case of Kocaeli (Izmit) Earthquake, August 17, 1999. *Remote Sensing of Environment*, **96**, 409-426. https://doi.org/10.1016/j.rse.2005.04.006

[14] Blackett, M., Wooster, M.J. and Malamud, B.D. (2011) Correction to "Exploring Land Surface Temperature Earthquake Precursors: A Focus on the Gujarat (India) Earthquake of 2001". *Geophysical Research Letters*, **38**, L18307. https://doi.org/10.1029/2011gl049428

[15] Shah, M., Khan, M., Ullah, H. and Ali, S. (2018) Thermal Anomalies Prior to the 2015 Gorkha (Nepal) Earthquake from Modis Land Surface Temperature and Outgoing Longwave Radiations. *Geodynamics & Tectonophysics*, **9**, 123-138. https://doi.org/10.5800/gt-2018-9-1-0341

[16] Piscini, A., De Santis, A., Marchetti, D. and Cianchini, G. (2017) A Multi-Parametric Climatological Approach to Study the 2016 Amatrice-Norcia (Central Italy) Earthquake Preparatory Phase. *Pure and Applied Geophysics*, **174**, 3673-3688. https://doi.org/10.1007/s00024-017-1597-8

[17] Draz, M.U., Shah, M., Jamjareegulgarn, P., Shahzad, R., Hasan, A.M. and Ghamry, N.A. (2023) Deep Machine Learning Based Possible Atmospheric and Ionospheric Precursors of the 2021 Mw 7.1 Japan Earthquake. *Remote Sensing*, **15**, Article 1904.

https://doi.org/10.3390/rs15071904

[18] Ghosh, S., Sasmal, S., Maity, S.K., Potirakis, S.M. and Hayakawa, M. (2024) Thermal Anomalies Observed during the Crete Earthquake on 27 September 2021. *Geosciences*, **14**, Article 73. https://doi.org/10.3390/geosciences14030073

[19] Ghosh, S., Chowdhury, S., Kundu, S., Sasmal, S., Politis, D.Z., Potirakis, S.M., *et al.* (2021) Unusual Surface Latent Heat Flux Variations and Their Critical Dynamics Revealed before Strong Earthquakes. *Entropy*, **24**, Article 23. https://doi.org/10.3390/e24010023

[20] Ouzounov, D., Liu, D., Chunli, K., Cervone, G., Kafatos, M. and Taylor, P. (2007) Outgoing Long Wave Radiation Variability from IR Satellite Data Prior to Major Earthquakes. *Tectonophysics*, **431**, 211-220. https://doi.org/10.1016/j.tecto.2006.05.042

[21] Venkatanathan, N. and Natyaganov, V. (2014) Outgoing Longwave Radiations as Pre-Earthquake Signals: Preliminary Results of 24 September 2013 M7.7 Earthquake. *Current Science*, **106**, 1291-1297.

[22] Xiong, P., Shen, X.H., Bi, Y.X., Kang, C.L., Chen, L.Z., Jing, F., *et al.* (2010) Study of Outgoing Longwave Radiation Anomalies Associated with Haiti Earthquake. *Natural Hazards and Earth System Sciences*, **10**, 2169-2178. https://doi.org/10.5194/nhess-10-2169-2010

[23] Shah, M., Ehsan, M., Abbas, A., Ahmed, A. and Jamjareegulgarn, P. (2022) Possible Thermal Anomalies Associated with Global Terrestrial Earthquakes during 2000-2019 Based on Modis-LST. *IEEE Geoscience and Remote Sensing Letters*, **19**, 1-5. https://doi.org/10.1109/lgrs.2021.3084930

[24] Zarchi, A.K.; Maharan, M.R.S. (2020) Fault Distance-Based Approach in Thermal Anomaly Detection before Strong Earthquakes. *Natural Hazards and Earth System Sciences*, 391. https://doi.org/10.5194/nhess-2020-391

[25] Genzano, N., Filizzola, C., Hattori, K., Pergola, N. and Tramutoli, V. (2021) Statistical Correlation Analysis between Thermal Infrared Anomalies Observed from MTSATs and Large Earthquakes Occurred in Japan (2005-2015). *Journal of Geophysical Research*: *Solid Earth*, **126**, e2020JB020108. https://doi.org/10.1029/2020jb020108

[26] Sharma, P., Bardhan, A., Kumari, R., Sharma, D.K. and Sharma, A.K. (2024) Variation of Surface Latent Heat Flux (SLHF) Observed during High-Magnitude Earthquakes. *The Journal of Indian Geophysical Union*, **28**, 131-142.

[27] De Santis, A., Balasis, G., Pavón-Carrasco, F.J., Cianchini, G. and Mandea, M. (2017) Potential Earthquake Precursory Pattern from Space: The 2015 Nepal Event as Seen by Magnetic Swarm Satellites. *Earth and Planetary Science Letters*, **461**, 119-126. https://doi.org/10.1016/j.epsl.2016.12.037

[28] De Santis, A., Cianchini, G., Marchetti, D., Piscini, A., Sabbagh, D., Perrone, L., *et al.* (2020) A Multiparametric Approach to Study the Preparation Phase of the 2019 M7.1 Ridgecrest (California, United States) Earthquake. *Frontiers in Earth Science*, **8**, Article 540398. https://doi.org/10.3389/feart.2020.540398

[29] Akhoondzadeh, M., De Santis, A., Marchetti, D., Piscini, A. and Jin, S. (2019) Anomalous Seismo-LAI Variations Potentially Associated with the 2017 Mw = 7.3 Sarpol-E Zahab (Iran) Earthquake from Swarm Satellites, GPS-TEC and Climatological Data. *Advances in Space Research*, **64**, 143-158. https://doi.org/10.1016/j.asr.2019.03.020

[30] Ouzounov, D., Pulinets, S., Davidenko, D., Rozhnoi, A., Solovieva, M., Fedun, V., *et al.* (2021) Transient Effects in Atmosphere and Ionosphere Preceding the 2015 M7.8 and M7.3 Gorkha-Nepal Earthquakes. *Frontiers in Earth Science*, **9**, Article 757358. https://doi.org/10.3389/feart.2021.757358

[31] Parrot, M., Tramutoli, V., Liu, T.J.Y., Pulinets, S., Ouzounov, D., Genzano, N., *et al.* (2021) Atmospheric and Ionospheric Coupling Phenomena Associated with Large Earthquakes. *The European Physical Journal Special Topics*, **230**, 197-225. https://doi.org/10.1140/epjst/e2020-000251-3

[32] Sasmal, S., Chowdhury, S., Kundu, S., Politis, D.Z., Potirakis, S.M., Balasis, G., *et al.* (2021) Pre-Seismic Irregularities during the 2020 Samos (Greece) Earthquake (M = 6.9) as Investigated from Multi-Parameter Approach by Ground and Space-Based Techniques. *Atmosphere*, **12**, Article 1059. https://doi.org/10.3390/atmos12081059

[33] Hayakawa, M., Izutsu, J., Schekotov, A., Yang, S., Solovieva, M. and Budilova, E. (2021) Lithosphere-Atmosphere-Ionosphere Coupling Effects Based on Multiparameter Precursor Observations for February-March 2021 Earthquakes (M~7) in the Offshore of Tohoku Area of Japan. *Geosciences*, **11**, Article 481. https://doi.org/10.3390/geosciences11110481

[34] Hayakawa, M., Schekotov, A., Izutsu, J., Yang, S., Solovieva, M. and Hobara, Y. (2022) Multi-Parameter Observations of Seismogenic Phenomena Related to the Tokyo Earthquake (M = 5.9) on 7 October 2021. *Geosciences*, **12**, Article 265. https://doi.org/10.3390/geosciences12070265

[35] D'Arcangelo, S., Regi, M., De Santis, A., Perrone, L., Cianchini, G., Soldani, M., *et al.* (2023) A Multiparametric-Multilayer Comparison of the Preparation Phase of Two Geophysical Events in the Tonga-Kermadec Subduction Zone: The 2019 M7.2 Kermadec Earthquake and 2022 Hunga Ha'apai Eruption. *Frontiers in Earth Science*, **11**, Article 1267411. https://doi.org/10.3389/feart.2023.1267411

[36] Zhang, X., Liu, J., De Santis, A., Perrone, L., Xiong, P., Zhang, X., *et al.* (2023) Lithosphere-Atmosphere-Ionosphere Coupling Associated with Four Yutian Earthquakes in China from GPS TEC and Electromagnetic Observations Onboard Satellites. *Journal of Geodynamics*, **155**, Article 101943. https://doi.org/10.1016/j.jog.2022.101943

[37] Marchetti, D., Zhu, K., Piscini, A., Ghamry, E., Shen, X., Yan, R., *et al.* (2024) Changes in the Lithosphere, Atmosphere, and Ionosphere before and during the Mw = 7.7 Jamaica 2020 Earthquake. *Remote Sensing of Environment*, **307**, Article 114146. https://doi.org/10.1016/j.rse.2024.114146

[38] Hayakawa, M. and Hobara, Y. (2024) Integrated Analysis of Multi-Parameter Precursors to the Fukushima Offshore Earthquake (Mj = 7.3) on 13 February 2021 and Lithosphere-Atmosphere-Ionosphere Coupling Channels. *Atmosphere*, **15**, Article 1015. https://doi.org/10.3390/atmos15081015

[39] Sasmal, S., Chowdhury, S., Kundu, S., Ghosh, S., Politis, D., Potirakis, S., *et al.* (2023) Multi-Parametric Study of Seismogenic Anomalies during the 2021 Crete Earthquake (M = 6.0). *Annals of Geophysics*, **66**, SE646. https://doi.org/10.4401/ag-8992

[40] Cianchini, G., Calcara, M., De Santis, A., Piscini, A., D'Arcangelo, S., Fidani, C., *et al.* (2024) The Preparation Phase of the 2023 Kahramanmaraş (Turkey) Major Earthquakes from a Multidisciplinary and Comparative Perspective. *Remote Sensing*, **16**, Article 2766. https://doi.org/10.3390/rs16152766

[41] Hayakawa, M., Hirooka, S., Michimoto, K., Potirakis, S.M. and Hobara, Y. (2025) Meteorological Anomalies during Earthquake Preparation: A Case Study for the 1995 Kobe Earthquake (M = 7.3) Based on Statistical and Machine Learning-Based Analyses. *Atmosphere*, **16**, Article 88. https://doi.org/10.3390/atmos16010088

[42] Varotsos, P.A., Sarlis, N.V. and Skordas, E.S. (2011) Natural Time Analysis: The New View of Time, Precursory Seismic Electric Signals, Earthquakes and other Complex Time Series. Springer. https://doi.org/10.1007/978-3-642-16449-1

[43] Eftaxias, K., Potirakis, S.M. and Contoyiannis, Y. (2018) Four-Stage Model of Earth-

quake Generation in Terms of Fracture-Induced Electromagnetic Emissions. In: Chelidze, T., Vallianatos, F. and Telesca, L., Eds., *Complexity of Seismic Time Series*, Elsevier, 437-502. https://doi.org/10.1016/b978-0-12-813138-1.00013-4

[44] Potirakis, S.M., Karadimitrakis, A. and Eftaxias, K. (2013) Natural Time Analysis of Critical Phenomena: The Case of Pre-Fracture Electromagnetic Emissions. *Chaos*: *An Interdisciplinary Journal of Nonlinear Science*, **23**, Article 023117. https://doi.org/10.1063/1.4807908

[45] Potirakis, S., Asano, T. and Hayakawa, M. (2018) Criticality Analysis of the Lower Ionosphere Perturbations Prior to the 2016 Kumamoto (Japan) Earthquakes as Based on VLF Electromagnetic Wave Propagation Data Observed at Multiple Stations. *Entropy*, **20**, Article 199. https://doi.org/10.3390/e20030199

[46] Potirakis, S.M., Contoyiannis, Y., Schekotov, A., Eftaxias, K. and Hayakawa, M. (2021) Evidence of Critical Dynamics in Various Electromagnetic Precursors. *The European Physical Journal Special Topics*, **230**, 151-177. https://doi.org/10.1140/epjst/e2020-000249-x

[47] Yang, S., Potirakis, S.M., Sasmal, S. and Hayakawa, M. (2020) Natural Time Analysis of Global Navigation Satellite System Surface Deformation: The Case of the 2016 Kumamoto Earthquakes. *Entropy*, **22**, Article 674. https://doi.org/10.3390/e22060674

[48] Ghosh, S., Chowdhury, S., Kundu, S., Sasmal, S., Politis, D.Z., Potirakis, S.M., *et al.* (2021) Unusual Surface Latent Heat Flux Variations and Their Critical Dynamics Revealed before Strong Earthquakes. *Entropy*, **24**, Article 23. https://doi.org/10.3390/e24010023

[49] Politis, D.Z., Potirakis, S.M., Contoyiannis, Y.F., Biswas, S., Sasmal, S. and Hayakawa, M. (2021) Statistical and Criticality Analysis of the Lower Ionosphere Prior to the 30 October 2020 Samos (Greece) Earthquake (M6.9), Based on VLF Electromagnetic Propagation Data as Recorded by a New VLF/LF Receiver Installed in Athens (Greece). *Entropy*, **23**, Article 676. https://doi.org/10.3390/e23060676

[50] Politis, D.Z., Potirakis, S.M., Kundu, S., Chowdhury, S., Sasmal, S. and Hayakawa, M. (2022) Critical Dynamics in Stratospheric Potential Energy Variations Prior to Significant (M > 6.7) Earthquakes. *Symmetry*, **14**, Article 1939. https://doi.org/10.3390/sym14091939

[51] Schekotov, A., Borovleva, K., Pilipenko, V., Chebrov, D. and Hayakawa, M. (2023) Meteorological Response of Kamchatka Seismicity. In: Kosterov, A., Lyskova, E., Mironova, I., Apatenkov, S. and Baranov, S., Eds., *Springer Proceedings in Earth and Environmental Sciences*, Springer International Publishing, 237-247. https://doi.org/10.1007/978-3-031-40728-4_17

[52] Virk, H.S. and Singh, B. (1994) Radon Recording of Uttarkashi Earthquake. *Geophysical Research Letters*, **21**, 737-740. https://doi.org/10.1029/94gl00310

[53] Heinicke, J., Koch, U. and Martinelli, G. (1995) CO_2 and Radon Measurements in the Vogtland Area (Germany)—A Contribution to Earthquake Prediction Research. *Geophysical Research Letters*, **22**, 771-774. https://doi.org/10.1029/94gl03074

[54] Tsunogai, U. and Wakita, H. (1996) Anomalous Changes in Groundwater Chemistry. Possible Precursors of the 1995 Hyogo-Ken Nanbu Earthquake, Japan. *Journal of Physics of the Earth*, **44**, 381-390. https://doi.org/10.4294/jpe1952.44.381

[55] Igarashi, G., Saeki, S., Takahata, N., Sumikawa, K., Tasaka, S., Sasaki, Y., *et al.* (1995) Ground-Water Radon Anomaly before the Kobe Earthquake in Japan. *Science*, **269**, 60-61. https://doi.org/10.1126/science.269.5220.60

[56] Yasuoka, Y., Igarashi, G., Ishikawa, T., Tokonami, S. and Shinogi, M. (2006) Evidence of Precursor Phenomena in the Kobe Earthquake Obtained from Atmospheric Radon

Concentration. *Applied Geochemistry*, **21**, 1064-1072. https://doi.org/10.1016/j.apgeochem.2006.02.019

[57] Varotsos, P.A., Sarlis, N.V. and Skordas, E.S. (2001) Spatio-Temporal Complexity Aspects on the Interrelation between Seismic Electric Signals and Seismicity. *Praktika of the Academy of Athens*, **76**, 294-321.

[58] Varotsos, P.A., Sarlis, N.V. and Skordas, E.S. (2002) Long-Range Correlations in the Electric Signals That Precede Rupture. *Physical Review E*, **66**, Article 059902. https://doi.org/10.1103/physreve.66.011902

[59] Varotsos, P.A., Sarlis, N.V., Tanaka, H.K. and Skordas, E.S. (2005) Similarity of Fluctuations in Correlated Systems: The Case of Seismicity. *Physical Review E*, **72**, Article 041103. https://doi.org/10.1103/physreve.72.041103

[60] Abe, S., Sarlis, N.V., Skordas, E.S., Tanaka, H.K. and Varotsos, P.A. (2005) Origin of the Usefulness of the Natural-Time Representation of Complex Time Series. *Physical Review Letters*, **94**, Article 170601. https://doi.org/10.1103/physrevlett.94.170601

[61] Varotsos, P.A., Sarlis, N.V., Skordas, E.S., Tanaka, H.K. and Lazaridou, M.S. (2006) Entropy of Seismic Electric Signals: Analysis in Natural Time under Time Reversal. *Physical Review E*, **73**, Article 031114. https://doi.org/10.1103/physreve.73.031114

[62] Sarlis, N.V., Skordas, E.S. and Varotsos, P.A. (2011) Similarity of Fluctuations in Systems Exhibiting Self-Organized Criticality. *Europhysics Letters*, **96**, Article 28006. https://doi.org/10.1209/0295-5075/96/28006

[63] Sarlis, N.V., Skordas, E.S., Lazaridou, M.S. and Varotsos, P.A. (2008) Investigation of Seismicity after the Initiation of a Seismic Electric Signal Activity until the Main Shock. *Proceedings of the Japan Academy, Series B*, **84**, 331-343. https://doi.org/10.2183/pjab.84.331

[64] Hayakawa, M., Hobara, Y., Michimoto, K. and Nickolaenko, A.P. (2024) The Generation of Seismogenic Anomalous Electric Fields in the Lower Atmosphere, and Its Application to Very-High-Frequency and Very-Low-Frequency/Low-Frequency Emissions: A Review. *Atmosphere*, **15**, Article 1173. https://doi.org/10.3390/atmos15101173

[65] Pulinets, S. and Budnikov, P. (2022) Atmosphere Critical Processes Sensing with ACP. *Atmosphere*, **13**, Article 1920. https://doi.org/10.3390/atmos13111920

[66] Pulinets, S., Budnikov, P., Karelin, A. and Žalohar, J. (2023) Thermodynamic Instability of the Atmospheric Boundary Layer Stimulated by Tectonic and Seismic Activity. *Journal of Atmospheric and Solar- Terrestrial Physics*, **246**, Article 106050. https://doi.org/10.1016/j.jastp.2023.106050

[67] Shitov, A.V., Pulinets, S.A. and Budnikov, P.A. (2023) Effect of Earthquake Preparation on Changes in Meteorological Characteristics (Based on the Example of the 2003 Chuya Earthquake). *Geomagnetism and Aeronomy*, **63**, 395-408. https://doi.org/10.1134/s0016793223600285

[68] Ghosh, S., Sasmal, S., Maity, S.K., Potirakis, S.M. and Hayakawa, M. (2024) Thermal Anomalies Observed during the Crete Earthquake on 27 September 2021. *Geosciences*, **14**, Article 73. https://doi.org/10.3390/geosciences14030073